JASA EXPRESS LETTERS ARTICLE asa.scitation.org/journal/jel

Design and simulation of acoustic vortex wave arrays for long-range underwater communication

Mark E. Kelly and Chengzhi Shi[a)]
George W. Woodruff School of Mechanical Engineering, Georgia Institute of Technology, Atlanta, Georgia 30332, USA
mkelly75@gatech.edu, chengzhi.shi@gatech.edu

Abstract: The formation and propagation of acoustic vortex waves have been of increasing interest for multiple applications, namely, underwater acoustic communications. Several methods have been presented to form these vortices in underwater environments; however, their performance and propagation over long distances is largely unstudied. Understanding the long-distance propagation of these waves is vital to enhancing their usefulness as an added degree of freedom in underwater acoustic communications systems. In this work, the ray tracing algorithm of BELLHOP is used to investigate the design parameters of vortex wave transducer and receiver arrays consisting of multiple rings of independently controlled transducers and simulate their performance.

[Editor: Gopu R Potty] https://doi.org/10.1121/10.0019884

Received: 27 April 2023 **Accepted:** 7 June 2023 **Published Online:** 5 July 2023

1. Introduction

The underwater acoustic communication environment is both complex and challenging. While radio frequency waves meet the needs of high-speed communications in air, they attenuate rapidly underwater due to absorption and their propagation is limited to centimeters.[1–4] Acoustic waves, on the other hand, are capable of propagating long distances in underwater environments. Even so, the available bandwidth is still limited severely to tens of kHz by attenuation at a kilometer scale,[5] which causes bottlenecks in underwater acoustics communications channels. Several methods of data transfer have been established for underwater acoustic communications systems,[6–17] with data rate peaking at approximately 40 kb/s (for comparison, 4 G LTE data peaks at 40 Mb/s). These methods rely primarily on temporal and frequency modulation techniques. This disparity highlights the currently unmet need for high-speed communications methods in underwater acoustic applications.

One method of easing the bottleneck and increasing data rate in underwater acoustic communications systems is to explore further potential degrees of freedom that exist within acoustic waves. Acoustic orbital angular momentum (OAM) is a physical quantity characterizing the rotation of the pressure wavefront in acoustic vortex waves.[18] These vortex waves carry unique spiral-shaped phase patterns which are characterized by the amount of rotation in a given pressure field. This characteristic is termed topological charge, and is represented by an integer *l*. Shi *et al.* have presented a method of forming OAM carrying waves and has also demonstrated that their topological charges form an orthogonal basis set which can be multiplexed and demultiplexed.[19] In Fan *et al.*, the authors presented a method of using the BELLHOP ray tracing algorithm to track the dominant features of a propagating OAM carrying vortex wave in underwater acoustic environments.[20] Their exploration, however, is limited to a single array comprised of a ring of eight transducers. Larger arrays consisting of more transducers which provide an increase in both directivity and available OAM charges are required for the practical implementation of OAM-based underwater acoustic communications systems. This work, therefore, employs these established methods to explore the performance of various array designs over useful ranges for underwater acoustic communications systems in multiple environments and proposes the design parameters for a prototype useful up to 1 km.

2. Methods and results

2.1 Generation of OAM carrying vortex waves

While BELLHOP is capable of simulating three-dimensional propagation, the resolution required to resolve the full detail in the OAM wavefront is too high to make this approach practical as an array design tool. Similarly, finite element methods are computationally limited for assessing long range propagation of these waves. Instead, two-dimensional simulations are used by employing the methods described in Fan *et al.*[20] Each source in the vortex-wave producing array is simulated as a

[a)]Also at: Parker H. Petit Institute for Bioengineering and Bioscience, Georgia Institute of Technology, Atlanta, GA 30332, USA. Author to whom correspondence should be addressed.

point source at its respective position in the water column. The individual pressure fields are adjusted to account for the phase offsets between the source transducers and coherently summed to yield the resultant pressure field for the propagating vortex wave. Given the known amplitude and phase characteristics of the wavefront, it is possible to track the dominant features of the propagating vortex wave as it traverses the space.

The phase relationships between successive transducers in a single ring are given by $\theta = 2\pi l/N$, where l is the topological charge and N represents the number of transducers in a given ring.[19] The number of achievable charges by a given ring of transducers is limited by the Nyquist criteria, which states that a wave must be sampled at least twice per cycle for a faithful reconstruction. This translates to a minimum of $(2L + 1)$ transducers per ring to produce a maximum topological charge of L. A ring of 16 transducers will therefore be able to achieve a charge of ± 7. For multiple rings, the phase relationships are determined by following the Bessel function $\theta = J_0(kr)e^{i\varphi l}$, where k represents the in-plane wave number and the source is located at the polar coordinates (r, φ). This gives an aperture-limited approximation of a Bessel beam. Figure 1 depicts this relationship for a hypothetical array consisting of three concentric rings of 16 transducers spaced 5 wavelengths apart where $l = \pm 1$ and shows the resulting pressure wave front. The rings are oriented such that transducers from successive rings are placed along the same radial line for simplicity of design, though provided the appropriate phase offset is applied, the rotation of the rings relative to each other will have no impact.

It is apparent in the pressure field that significant energy is lost to the interference pattern surrounding the central vortex. In theory, these beams should approximate an acoustic Bessel beam, meaning no diffraction should be observed, however, due to the limited aperture size, the long range over which the propagation is considered, and the fact that the medium is not well approximated by an infinite free space, diffraction will in fact occur.[21] The effects of this are apparent in the corresponding BELLHOP simulation depicted in Fig. 2(a). The BELLHOP simulations are conducted for a deep-water environment (5000 m) with the Munk sound speed profile (SSP).[22] As an effect of the limited aperture size, the energy loss is too large to allow for long-range propagation of the vortex wave, making this array design untenable. Significant improvement is observed, however, by simply maintaining transducers along a radial line in phase. This results in less energy being lost to the off-axis elements of the vortex wave formation. The differences in the formation of the OAM-carrying vortex wave are discussed in greater detail in the SI.

With this improvement, these methods can be utilized to explore more array geometries and improve efficiency and directionality.

2.2 Effects of increasing array size and number of transducers

As with conventional circular arrays, the directivity of vortex-wave producing circular arrays improves as array size increases. Figure 3 shows the resultant pressure field at distances of 100 and 1000 m after increasing array size from rings with radii of 5, 10, and 15 wavelengths to radii of 15, 20, and 25 wavelengths. This figure also conveys the evolution and deformation of the vortex as it propagates through the medium. By 1000 m, the vortex is in-tact (as is evident through the phase relationship plot), however, a deformation in the phase is evident. Any deformation in phase represents a potential complication in deconvolution of OAM based communications. These results, in addition to those of Fan *et al.*,[20] point towards the sensitivity of vortices as they traverse long distances in inhomogeneous media. As is the case for all underwater acoustic systems, understanding environmental conditions will play a vital role while operating OAM-based communications systems in the field. (Of note: the apparent sharp, horizontal discontinuities in the amplitude plots at 1000 m in

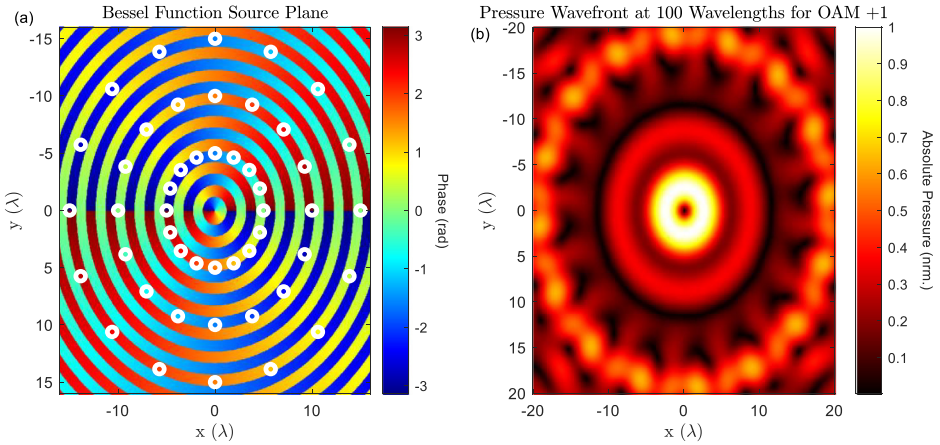

Fig. 1. Generation of OAM +1 with an active transducer array (a) The layout and phase relationship between transducers (shown as white circles) to produce OAM +1, (b) The resultant pressure wave front evaluated at 100 wavelengths from the source array. Wavelength is calculated using a reference sound speed of 1500 m/s in water.

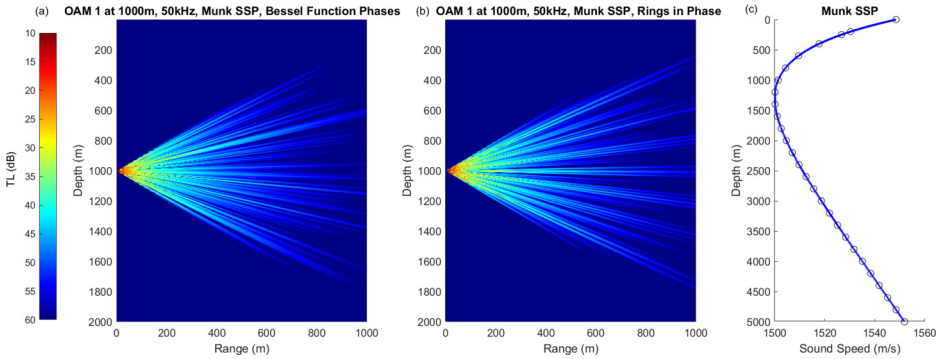

Fig. 2. Propagation of OAM carrying waves in deep water with the Munk SSP (a) Vortex wave propagation resulting from maintaining the three rings in phase (b) Vortex wave propagation resulting from maintaining the three rings in phase (c) the Munk SSP. It is important to note that the vortex wave is represented by the central beam.

depth are likely an artifact of the ray tracing algorithm which occur as a result of the sound speed profile being explicitly defined at this point.)

Table 1 lists the directivity of OAM 1 for multiple arrays, representing a range of sizes and geometries. Given that the array being presented is expected to be useful in both lab and field environments, and that to be realistically realizable, economic and materials considerations should be accounted for, some concessions must be made. Over the ranges considered here the improvements in directivity (as represented by beam width at 1 km) do not justify the increase in array size far beyond an array with radii of 15, 20, and 25 wavelengths (the resulting array will have a diameter of approximately 1.8 m). Similarly, there is little benefit to adding more rings of transducers. Figures representing these relationships can be found in the supplemental information.[23]

This analysis suggests that an array consisting of three rings located at radii of 15, 20, and 25 wavelengths, each with 16 transducers is sufficient for OAM-based communications arrays up to at least 1 km. Furthermore, at 50 kHz, a radius of 25 wavelengths equates to an array radius of 0.75 m which is realistically realizable for potential use on both manned and unmanned systems. It is important to note that the array proposed here is not intended to represent the sole solution to all array optimization problems; rather, it represents an array which is realistically feasible for fabrication,

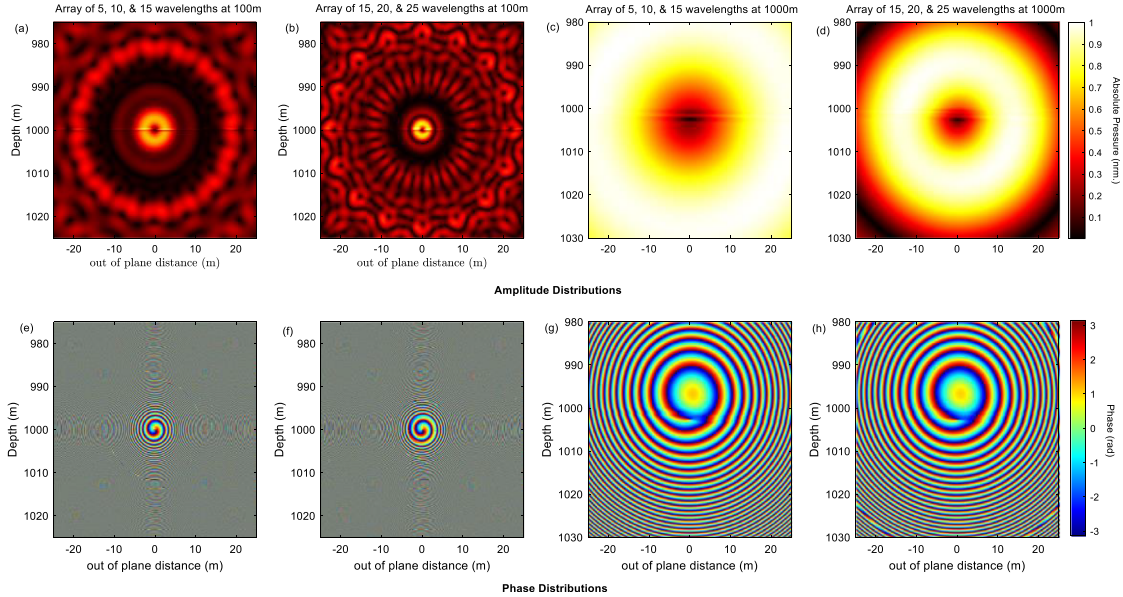

Fig. 3. Amplitude and phase distributions for two different arrays at ranges of 100 and 1000 m. (a), (e) The resultant wave front generated by an array consisting of three rings placed at 5, 10, and 15 wavelengths at 100 m. (b), (f) The resultant wave front generated by an array consisting of three rings placed at 15, 20, and 25 wavelengths at 100 m. (c), (g) The resultant wave front generated by an array consisting of three rings placed at 5, 10, and 15 wavelengths at 1000 m. (d), (h) The resultant wave front generated by an array consisting of three rings placed at 15, 20, and 25 wavelengths at 1000 m. This increase results in a physically realizable transmitter array with a radius of 75 m at 50 kHz with sufficient directivity to be useful to and beyond ranges of 1 km.

Table 1. The performance of a representative selection of potential arrays (OAM 1).

Ring radii (wavelengths)	Transducers per ring	Approximate beam width at 1 km (m)
5, 10, 15	16	50
15, 20, 25	16	20
15, 20, 25	24	20
15, 20, 25, 30	16	20
30, 40, 50	16	14
30, 40, 50, 60	16	12

useful in lab and field environments, and is cost-effective. The principles and methods presented here represent a repeatable framework which may be adapted to more specific applications.

2.3 Multipath propagation

At short propagation ranges or in deep water, the direct path will dominate, and the refraction and reflection of acoustic rays traversing the bulk of the water column will have a minimal effect. However, performance of OAM communications systems over long range and in shallower environments is also of critical importance for numerous applications. Figure 4 presents the performance of the array discussed in Sec. 2.2 in two multipath scenarios, and the resulting implications are discussed below.

2.3.1 Long-range propagation

At the ranges explored so far, reflection and refraction of rays traversing the water column has had minimal effect. Long-range propagation, being of interest for numerous applications must also be explored. Figure 4(a) depicts the performance of the same array presented in Sec. 2.2 over longer ranges. Predictably, as range increases, the propagation becomes more complicated. The relaxing of the vortex, coupled with interference from the reflections and refraction of the side lobes indicates that significant issues may be present. Despite the improvements in directivity over the arrays presented in the earlier works referenced,[19,20] the difficulties explored in Fan *et al.*[20] are not significantly improved upon for ranges far beyond 1 km.

2.3.2 Shallow water propagation

The multipath transmission that arises in shallower water leads to similar issues of interference as with long range propagation in deep water. Figure 4(b) depicts a hypothetical case for a vortex-wave-producing array in an environment with 600 m depth. The central beam carrying the vortex, however, remains intact at short ranges in these environments. Furthermore, the interference by the side-lobes can be clearly seen as off-axis when compared to the mainlobe. This suggests that a sufficiently directional receiver array and common k-space filtering techniques will be effective at recovering the appropriate information. The SSP here differs significantly from the Munk profile seen in deep water and is representative of one possibility which may be observed in shallow water where a warm surface layer creates downward refracting behavior in the upper section of the water column.

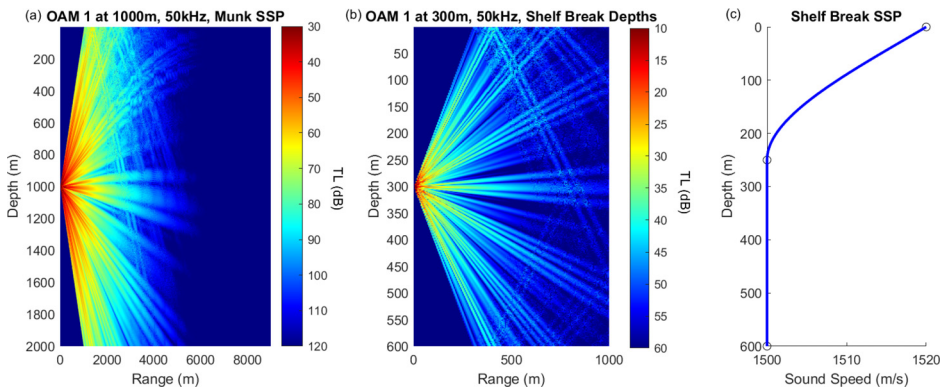

Fig. 4. Vortex waves propagating in two different scenarios with multipath propagation. (a) A vortex wave propagating over longer ranges in a deep water environment with the Munk SSP. (b) A vortex wave propagating over shorter ranges in a shallower water environment. (c) The sound speed profile for which Fig. 4(b) is simulated.

2.4 Considerations for receiver array design

Shi *et al.*[19] presented an exploration into the design principles of potential receiver arrays by exploring the relationship between receiver array geometry and number of transducers against the changes in perceived bit error rate at a distance of 100 wavelengths. Expanding those principles to account for the expansion of the central beam is vital to the employment of these systems. In the cases presented here, the resultant central beam diameter for OAM +1 is approximately 20 m at 1 km. With the full center beam captured by the receiver array, the relationship between the number of receivers and BER presented in Shi's work, should hold true. However, as topological charge increases, the size of the central beam increases as well, indicating that further analysis is required for the implementation of OAM-based communications systems in ocean environments. Arrays of sufficient size are readily achievable on larger vessels and submarines as well as in deployable (towed, fixed, or floating) arrays, however, exploration into the potential miniaturization of receiver arrays will be necessary for two-way communications on smaller manned and unmanned vessels.

3. Conclusion and future work

In summary, this work has presented an exploration into the behavior of vortex wave-producing acoustic arrays in ocean environments. Simulations performed using BELLHOP suggest that both transmitter and receiver arrays are practically realizable, and a prototype transmitter array design is presented which will be useful to ranges of at least 1 km under multiple environmental conditions. Work is ongoing for the physical design and fabrication of such an array which is intended for testing in both lab and field environments. Exploration into the design, performance, and miniaturization of receiver arrays for OAM based communications is also ongoing.

Acknowledgments

This work is supported by the Office of Naval Research under Grant No. N00014-22-1-2551.

References and links

[1]G. M. Hale and M. R. Querry, "Optical constants of water in the 200 nm to 200 μm wavelength region," Appl. Opt. **12**, 555–563 (1973).
[2]T. I. Quickenden and J. A. Irvin, "The ultraviolet absorption spectrum of liquid water," J. Chem. Phys. **72**, 4416–4428 (1980).
[3]S. G. Warren, "Optical constants of ice from the ultraviolet to microwave," Appl. Opt. **23**, 1206–1225 (1984).
[4]H. Buiteveld, J. H. M. Hakvoolt, and M. Donze, "Optical properties of pure water," Proc. SPIE Ocean Opt. **2285**, 174–183 (1994).
[5]N. Friedman, *The Naval Institute Guide to World Naval Weapon Systems* (Naval Institute Press, Annapolis, MD, 2006).
[6]A. Kaya and S. Yauchi, "An acoustic communication system for subsea robot," in *Proceedings of OCEANS'89* (1989), pp. 765–770.
[7]M. Suzuki and T. Sasaki, "Digital acoustic image transmission system for deep sea research submersible," in *Proceedings of OCEANS'92* (1992), pp. 567–570.
[8]G. Ayela and J. M. Coudeville, "TIVA: A long range, high baud rate image data acoustic transmission system for underwater applications," in *Proceedings of the Underwater Defence Technology Conference*, Paris, France (1991).
[9]A. Goalic, J. Labat, I. Truhuil, S. Saoudi, and D. Riouaten, "Toward a digital acoustic underwater phone," in *Proceedings of OCEANS'94* (1994), pp. III.489–III.494.
[10]J. Fischer, K. Bennett, S. Reible, J. Cafarella, and I. Yao, "A high rate, underwater acoustic data communications transceiver," in *Proceedings of OCEANS'92* (1992), pp. 571–576.
[11]S. Merriam and D. Porta, "DSP-based acoustic telemetry modems," Sea Technology (May, 1993).
[12]M. Johnson, D. Herold, and J. Catipovic, "The design and performance of a compact underwater acoustic network node," in *Proceedings of OCEANS'94* (1994), pp. III.467–III.471.
[13]R. Galvin and R. F. W. Coates, "Analysis of the performance of an underwater acoustic communication system and comparison with a stochastic model," in *Proceedings of OCEANS'94* (1994), pp. III.478–III.482.
[14]G. S. Howe, P. Tarbit, O. Hinton, B. Sharif, and A. Adams, "Sub-sea acoustic remote communications utilizing an adaptive receiving beam former for multipath suppression," in *Proceedings of OCEANS'94* (1994), pp. I.313–I.316.
[15]P. S. D. Tarbit, G. Howe, O. Hinton, A. Adams, and B. Sharif, "Development of a real-time adaptive equalizer for a high-rate underwater acoustic data communication link," in *Proceedings of OCEANS'94* (1994), pp. I.307–I.312.
[16]M. Stojanovic, J. Catipovic, and J. G. Proakis, "Adaptive multichannel combining and equalization for underwater acoustic communications," J. Acoust. Soc. Am. **94**, 1621–1631 (1993).
[17]M. Stojanovic, J. Catipovic, and J. G. Proakis, "Reduced-complexity multichannel processing of underwater acoustic communication signals," J. Acoust. Soc. Am. **98**, 961–972 (1995).
[18]B. T. Hefner and P. L. Marston, "An acoustic helical wave transducer with applications of alignment of ultrasound and underwater systems," J. Acoust. Soc. Am. **106**, 3313–3316 (1999).
[19]C. Shi, M. Dubois, Y. Wang, and X. Zhang, "High-speed acoustic communication by multiplexing orbital angular momentum," Proc. Natl. Acad. Sci. U.S.A. **114**, 7250–7253 (2017).
[20]F. Xudong, Z. Zou, and L. Zhang, "Acoustic vortices in inhomogeneous media," Phys. Rev. Res. **1**, 032014(R) (2019).
[21]J. Durnin, J. Miceli, and J. Eberly, "Diffraction-free beams," Phys. Rev. Lett. **58**(15), 1499-1501 (1987).
[22]W. Munk, "Sound channel in an exponentially stratified ocean, with application to SOFAR," J. Acoust. Soc. Am. **55**(2), 220–226 (1974).
[23]See supplementary material at https://doi.org/10.1121/10.0019884 for additional figures and further discussion of the arrays presented herein.